

SECONDARY CRATERS OF THE ORIENTALE BASIN. Dijun Guo^{1, 2, 3}, Jianzhong Liu¹, James W. Head III³,
¹Center for Lunar and Planetary Science, Institute of Geochemistry, Chinese Academy of Sciences, Guiyang 550081, China (liujianzhong@mail.gyig.ac.cn) ²University of Chinese Academy of Sciences, Beijing 100049, China ³Department of Earth, Environmental and Planetary Sciences, Brown University, Providence, RI 02912 USA. (james_head@brown.edu)

Introduction: Secondary craters are small craters (relative to the primary) produced by impact of high-velocity ejecta blocks during the excavation stage of the cratering event. Generally, secondary craters appear in patterns of clusters and chains arrayed radially to the primary crater. Their distribution can be used to address conditions at the impact site (angle, azimuth of incidence, etc.) of the primary crater to study the effect of several factors in the impact cratering process [1]. As a major factor in the contamination of accurate age determination using the superposed impact crater size-frequency distribution (SFD) method, secondary craters should be excluded from the dataset [2, 3]. However, secondaries often contribute significantly to the small crater population [4-6] and therefore, particularly for large craters and basins, it is necessary to understand the morphology and distribution of secondary craters.

Previous studies have documented the characteristics of secondaries of fresh small craters in the tens of kilometers diameter range (e.g., [7-12]). However, secondaries from basins and smaller craters are different in some aspects, for instance, the V-shaped “herring bone” [13] is rarer in basin secondaries [14].

Oriente basin is the youngest basin on the Moon, so it provides an opportunity to investigate original lunar basin morphology and related geologic units. Documenting Oriente secondary craters provides the possibility of understanding the more highly degraded secondary craters of older basins. The Hevelius Formation, which is interpreted to be the ejecta deposits of Oriente basin is associated with abundant secondary chains [14-16]. Wilhelms et al., (1978) identified 569 Oriente secondary craters in the size range 4.5 to 20 km and computed the size-frequency distribution, but the results and measurement precision were limited by the image quality [6]. Here we use new spacecraft data to reassess Oriente basin secondaries.

Methods and Data: Study area. Individual primary craters can create millions of secondaries [2], and the continuous ejecta deposits and continuous secondary crater facies of an impact crater generally have different radial extents in different azimuths because the incidence direction is rarely vertical [1, 17]. In addition, the frequency of later impact events is asymmetric, leading to different degrees of degradation in different directions. To best estimate the distribution and characteristics of Oriente secondaries, we selected the

most well-developed and well-preserved region northwest of Oriente basin to study the secondaries in this region (Fig. 1). The area of study region is 1.6×10^6 km² and is divided into 12 annuli with the widths equal to half of Oriente radius (232.5 km); thus the outmost boundary is 6 radii to Cordillera ring. The study area occupies 6.88% of the entire circular area, i.e., each of the annular sectors makes up 6.88% the area of the corresponding annulus, so that the identified secondary craters sample the same percentage area in each annulus.

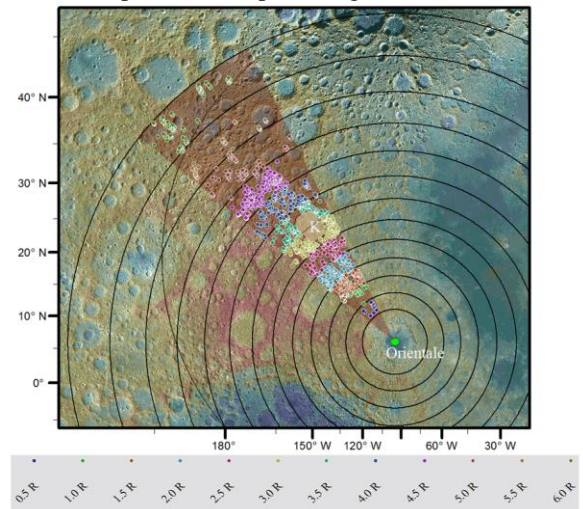


Fig. 1 Study region and secondary craters identified. The study area is brown-colored sector region outside the Cordillera ring. Crater in different colors represent the distance to Cordillera ring (R=Oriente radius). K- crater Kovalevskaya.

Criteria. Criteria for the recognition of secondary crater have been proposed by various workers (e.g., [5, 14, 18]). We follow the criteria established by previous analyses: (1) entrained within a chain, elongate crater group, and/or has a “herringbone” ejecta pattern; (2) shallower than primary impact craters; (3) highly elliptical with the long axis radial to Oriente basin center; (4) contains numerous interference features such as septa and mounds. An addition note for criteria (3) is that with the decreasing secondary crater size, the shapes are more subcircular.

Data and tools. Generally, we use LROC WAC images (100 m/pixel) and the LOLA DEM (1024 pixel/degree) to identify secondary craters. For cases where the geologic context is complicated, we used Kaguya images (20 m/pixel). The secondary craters are identified on ESRI ArcMap using Crater Helper Tools

(<http://astrogeology.usgs.gov/facilities/mrcrtr/gis-tools>) to map the craters and compute their diameters.

Results: We identify and map 1224 secondary craters in the study area (Fig. 1). However, Kovalevskaya, a superposed fresh crater in the sixth annular sector eliminated part of the secondaries in sixth and seventh annular sector (Fig. 1). By assuming a homogeneous secondary crater distribution in each annular sector, the total secondary crater number is 1321 after this correction. The statistics of 1224 Orientale secondary craters mapped yield a mean diameter of 8.55 km (standard deviation 4.94 km); the largest is 28.67 km, located in annular sector 1.5 radius from the Cordillera ring. The 25th percentile, median and 75th percentile are 4.87 km, 7.42 km and 11.51 km respectively.

The statistics and density of secondary craters in each annular sector are shown in Fig. 2. With increasing distance from Orientale basin, the secondary diameter decreases on average, as does the diameter of the largest secondary. The density is low at one radius from the basin rim, but increases to the largest beyond. The drop at 2.5 radius annular sector is influenced to some degree by formation of crater Kovalevskaya. Density decreases 3 radii outward. The increase at 6 radii may be caused by either widely distributed small crater clusters, which are possibly from Orientale, or by incorrectly identifying primary craters as secondary craters since the secondaries and small primaries are difficult to distinguish at this distance.

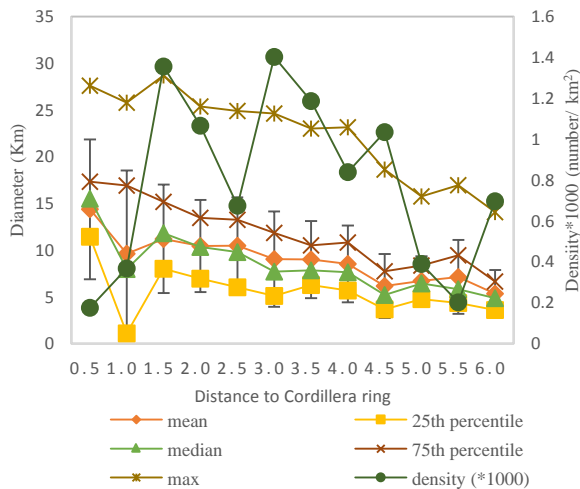


Fig. 2 Statistics of Orientale secondary craters in annular sectors. X-axis represents the multiple of Orientale radius from annular sector to the Cordillera ring. Standard deviations of mean secondary crater diameter are shown. Density in each annular sectors is multiplied by 1000.

As shown in Fig. 3, relatively larger Orientale secondary craters are mostly close to the basin rim, and their ratio in sectors decreases with increasing distance. Among the entire population of 1224 secondaries, crater diameters in the 3.54~8.62 km range are most

abundant (~45%), while secondaries larger than 13.69 km contribute only ~16%. For the very small secondaries, at least two factors can affect the ratio: (1) the age of primary impact, because they are more easily destroyed if formed earlier; (2) the resolution of images used to identify secondaries.

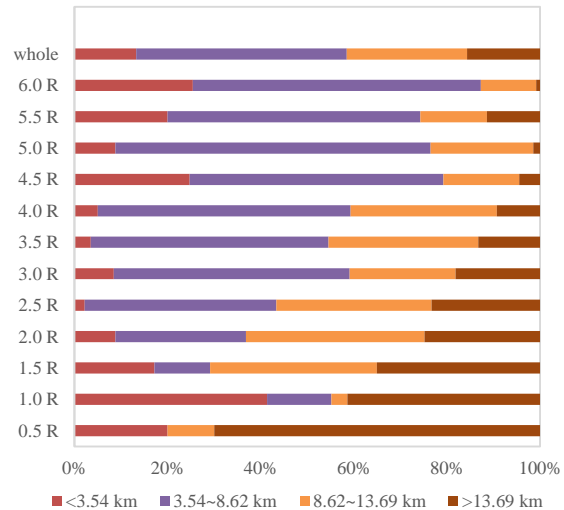


Fig. 3 The ratio of secondary craters within four diameter intervals in 12 annular sectors and as a whole.

Summary: This study identified 1224 secondary craters in the 1.6×10^6 km² region northwest of Orientale. The average secondary crater diameter is 8.55 km. By dividing the study area into 12 equal-distance (half-radius of Orientale) annular sectors, the distribution indicates that most of the large secondaries are close to the primary basin, and the diameter of largest secondary crater decreases with distance. The highest density secondary crater area is 1.5~3.5 radii from the basin rim. These relationships are now being tested elsewhere in the Orientale ejecta deposits and are being used to search for secondary populations around other more degraded basins.

References: [1] Xiao Z, et al.(2014) *Icarus*, 260-275.[2] McEwen A. S. and Bierhaus E. B.(2006) *Annu Rev Earth Pl Sc*, 535-567. [3] Neukum G. and Ivanov B. (1994) *Hazards due to Comets and Asteroids*. 359-416. [4] Bierhaus E., Chapman C. and Merline W. (2005) *Natur*, 7062, 1125- 1127. [5] Robbins S. and Hynek B. (2014) *EPSL*, 66-76. [6] Wilhelms D., Oberbeck V. and Aggarwal H. (1978), *9th LPSC*, 3735-3762. [7] Schultz P. and Singer J. (1980), *11th LPSC*, 2243-2259. [8] Dundas C. (2005), Salt Lake Annual Meeting. [9] Preblich B., McEwen A. and Studer D. (2005), *36th LPSC*, 2112. [10] Hirata N. and Nakamura A. (2006) *J GR-Planet*, E3. [11] Dundas C. and McEwen A. (2007) *Icarus*, 1, 31-40. [12] Pike R. (1972), 24th Interna. Geo. Con., 41-47. [13] Oberbeck V. and Morrison R. (1974) *The Moon* 415-455. [14] Wilhelms D. (1976), *7th LPSC*, 2883- 2901. [15] Mccauley J. (1967) *Geologic Atlas of the Moon*. [16] Head J., et al.(1993) *JGR-Planet*, E9, 17149-17181. [17] Robbins S. and Hynek B.(2011) *JGR-Planet*, E10003. [18] Shoemaker E. (1962) *Physics and Astronomy of the Moon*.